2007 IEEE International Conference on
Robotics and Automation
Roma, Italy, 10-14 April 2007

A Gas-Actuated Anthropomorphic Transhumeral Prosthesis

Kevin B. Fite, *Member, IEEE,* Thomas J. Withrow, Keith W. Wait, and Michael Goldfarb, *Member, IEEE*

Abstract— **This paper presents the design of an anthropomorphic 21 degree-of-freedom, 9 degree-of-actuation arm prosthesis for use by transhumeral amputees. The design leverages the power density of pneumatic actuation with the energy density of liquid propellants to obtain a self-powered dexterous prosthesis in which all of the requisite power, actuation, and sensing is packaged within the volumetric envelope of a normal human arm. Specifically, the arm utilizes a monopropellant as a gas generator to power nine pneumatic-type actuators that drive an elbow, three wrist degrees-of-freedom, and a 17 degree-of-freedom compliant hand. The design considerations discussed in this work include the design of compact, low-power servovalves; the choice of actuators based on energetic requirements of a normal arm; the design of compact elbow and wrist joints with integrated position and force sensing; and the components of the compliant hand design. The liquid-fueled prosthesis is expected to approach the dexterity of an anatomical arm and is projected to deliver half of the force and power output of an average human arm.**

I. Introduction

AMONG the many challenges that exist in the development of an anthropomorphic arm is that of providing a high number of actuated degrees-of-freedom, each capable of significant force and/or power, in a highly confined space. As such, a critical component of any viable approach to an anthropomorphic arm is the incorporation of actuators that deliver comparable power density, force density, strain capability, and bandwidth to human skeletal muscle, and importantly, must embody a similar form factor. In fact, since unlike a human arm, the geometric constraints of a transhumeral prosthesis requires that the elbow actuator lie in the forearm, comparable performance to a human will actually require greater power density than human skeletal muscle.

State-of-the-art electromagnetic motors have a reasonable power density and a good bandwidth, but they exhibit a low torque density (relatively to human joint actuation), and do not provide an appropriate form factor for high-density actuation in an anthropomorphic form. Due to their low torque density, an electromagnetic motor requires a significant transmission ratio, typically embodied by a gearhead. Use of a gearhead reduces significantly the power density of the actuator, due to both a reduction in efficiency and a corresponding increase in actuator weight (i.e., the gearhead both decreases the numerator and increases the denominator of the power density). The net result is an actuator with a power density that is approximately three to five times less than human skeletal muscle. The combined drawbacks of low power density and awkward form factor introduce significant challenges into the development of an electromagnetic motor actuated anthropomorphic arm with near-human capability. This paper describes an alternative means of developing an anthropomorphic arm based on a chemofluidic actuation approach. The proposed approach provides the actuator power density, force density, bandwidth, and form factor conducive to the development of an anthropomorphic arm, and also provides an improved energy density relative to state-of-the-art secondary (e.g., NiMH) batteries.

Manuscript received September 15, 2006. This work was supported in part by the U.S. Navy under Grant N66001-05-C-8045.

K. B. Fite is with Vanderbilt University, Nashville, TN 37235 USA (phone: 615-343-2782; fax: 615-343-6925; e-mail: kevin.fite@ vanderbilt.edu).

T. J. Withrow is with Vanderbilt University, Nashville, TN 37235 USA (e-mail: thomas.j.withrow@ vanderbilt.edu).

K. W. Wait is with Vanderbilt University, Nashville, TN 37235 USA (e-mail: keith.w.wait@ vanderbilt.edu).

M.Goldfarb is with Vanderbilt University, Nashville, TN 37235 USA (e-mail: michael.goldfarb@ vanderbilt.edu).

II. Description of the Chemofluidic Approach

The proposed approach is enabled by leveraging an actuation approach for compact self-powered systems recently developed by the authors [1-4]. This approach, which is based on the catalytic decomposition of the monopropellant hydrogen peroxide as an energy source, has recently been shown to provide a figure of merit for self-powered actuated systems that is an order of magnitude greater than state-of-the-art batteries and electromagnetic motors [2,4]. The authors have additionally demonstrated closed-loop position and force controlled versions of the monopropellant actuation approach with bandwidth appropriate for human movement. The catalytic reaction upon which the approach is based is strongly exothermic, and the resultant thermal energy is transduced to mechanical work via the expansion of the gaseous reaction products. Unlike non-catalytic combustion, this reaction scales downward well, essentially retaining its reaction efficiency even at very small scales. The catalytic reaction can in essence be considered a flow rate amplifier. Specifically, the propellant is stored in a pressured cartridge, which is pressured by a CO_2 cartridge. The proposed approach utilizes this pressurized propellant cartridge as the thermodynamic equivalent of a battery, with the output being a gas flow rate at a given pressure (rather than a current at a given voltage, as is the case with an electrical

battery). Just as with an electrical battery, the amount of output flow depends on the downstream impedance of the load. When the downstream impedance is infinite (i.e., no actuators in use and gas valves closed), the system will not draw any flow from the fuel cartridge (technically a propellant cartridge). When the downstream impedance is lowered (i.e., by one or several valves), pressure in the cartridge forces propellant through the catalyst, which effectively increases the flow rate from a signal level to a power level (i.e., through its exothermic release of heat and resulting gaseous expansion). The effective increase in flow rate is typically two to three orders of magnitude, and depends specifically on the concentration of propellant and the downstream pressure. The pressurized gas output is used to power a set of gas actuators, wherein the gas flow for each is controlled via a four-way servovalve. This configuration is depicted schematically in Fig. 1.

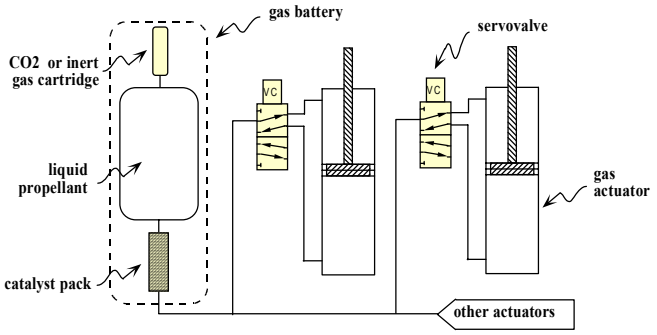

Fig. 1. Schematic diagram of proposed actuator configuration.

The development of gas-actuated prostheses is not without precedence, having been investigated in the 1960s and 1970s [5]. These devices used CO_2 tanks as power sources for pneumatically actuated arm prostheses. The control valves used were on/off valves actuated by external force commands from the amputee. Continued evolution of these systems was impeded by two major constraints. While CO_2 tanks provide a convenient means of gas generation, their relatively low energy density provides significant limitations to operating times before tank replacement is required (lifetimes on the order of 2-3 hours). Precision control of the pneumatic arms proved to be another significant impediment to their continued development. Attempts to implement closed-loop servo control of pneumatic prostheses suffered from the presence of limit cycles and instabilities in the closed-loop response that prevented accurate trajectory tracking [6].

The ongoing work presented in this paper improves upon the earlier devices by using monopropellants as the energy source and leveraging the demonstrated ability to obtain precision feedback control of such liquid-fueled systems [1-4]. With respect to the energetic characteristics, CO_2 has a volumetric energy density of 58 kJ/L. In comparison, 70% H_2O_2 possesses a volumetric energy density of 273 kJ/L. Because the monopropellant decomposition involves the breaking of molecular bonds, rather than the simple phase change associated with CO_2, the energy density improves significantly. The increased energy density of H_2O_2 (a factor of almost five) provides the capability of significantly increased operation times relative to CO_2-powered systems. For a given energetic output, the monopropellant-powered system will require 20% of the fuel volume required of the CO_2-powered system. Alternatively stated, for comparable fuel tank volume and energetic output, the H_2O_2-powered system will be able to operate five times longer than the CO_2-powered system.

In addition to the energetic characteristics that enable the development of an anthropomorphic arm with human-scale output capabilities, the proposed actuation approach also provides advantages with respect to the behavioral characteristics and control of the arm. Specifically, the proposed configuration exhibits an open-loop stiffness and damping similar to the human system, provides a degree of backdrivability similar to the human, requires no power consumption for isometric contractions, and can enable the control of joint impedance independently of joint torque. With regard to the last point, humans rely on the independent control of joint impedance and torque in order to adapt to interaction with various environments. Specifically, when interacting with a kinematic constraint, such as when opening a door or a drawer, the human will generate joint torques required for a given motion with a low output impedance, so that human arm will in essence follow the kinematic constraint dictated by the environment (i.e., the arc dictated by the door, or the linear path dictated by the prismatic joint of the drawer). In the absence of an externally imposed kinematic constraint, and in the case when the human would like to dictate the kinematics of the motion, such as when writing with a pen or cutting with a knife, the human will generate the joint torques required for the desired motion with a high output impedance. In the absence of variable output impedance, the human will have great difficulty in either interacting with one type of environment or the other. The ability to control open-loop output impedance (actually stiffness) independently of force at high bandwidth has been experimentally demonstrated by the authors, and is described in [7]. Note, however, that such independent control of torque and stiffness requires a pair of valves for each actuator, rather than the use of a single (4-way) valve. The current implementation of the arm (as subsequently described) includes only one valve per actuator, and thus does not afford the independent control of torque and stiffness. Despite this, by adding another valve at selected actuators, subsequent versions of the arm could include such behavior at selected joints.

In a manner conceptually similar to the energy conversion in skeletal muscle, use of a liquid fuel enables the direct chemical to mechanical energy conversion that enables the aforementioned actuator characteristics, which in turn enable the development of a high degree-of-freedom

anthropomorphic arm. Use of a liquid fuel, however, also brings with it some disadvantages, most notably (1) production of exhaust products, (2) some degree of audible noise associated with the exhaust, (3) elevated internal reaction temperatures, and (4) increased difficulty in packaging relative to a solid energy source such as a battery. Due to the inherently safe nature of the propellant (in concentrations less than 80%), in combination with proper design attention, these issues can be rendered inconsequential. Specifically, with regard to the safety of the propellant, hydrogen peroxide at the proposed concentration levels (70-80%) is completely nonflammable, insensitive to shock, has no possibility of detonation, and has completely safe reaction products (oxygen and steam). Despite this, the propellant is a strong oxidizer, and as such is best distributed in sealed cartridges for consumer distribution, much like CO_2 or propane. Regarding the gas temperature, though clearly elevated internally, the temperature is as low as can be achieved for a given energetic output, and is well within an acceptable range once exhausted from the actuators. With regard to the former, the energetic figure of merit for all exothermic reactions in which mechanical energy is extracted through (approximately) isothermal expansion is the ratio of the adiabatic reaction (or combustion) temperature to the molecular weight of the reaction product. As such, for a given energy density, the lower the molecular weight of the products, the lower the required reaction temperature. Second to hydrazine, hydrogen peroxide has the lowest molecular weight reaction product (approximately 23 kg/kg-mol), which means that the reaction temperatures are as low as one can achieve for a given energy density (excluding hydrazine, which is wholly inappropriate for consumer distribution). With regard to the exhaust temperature, though the adiabatic reaction temperature (i.e., the temperature prior to any extraction of work or heat loss) at the catalyst pack is relatively high (230 C for 70% peroxide), the gas temperature is quickly cooled as it expands through the actuator and performs work. Though the exact exhaust temperature depends on the motion and load, all prior experimental experience (with many types of loads and motions) indicates the exhaust temperature is comfortable for prolonged human exposure (i.e., one can hold one's hand one inch from the exhaust outlet continuously during operation). With regard to the audible output, the sound level of an elbow actuator curling an 11 kg (25 lb) weight at one Hertz was measured at 55 dB from one meter away (which is considered ambient), without any attempt to muffle or attenuate the sound. Thus, with a presumably lower power output, and with minor attempts to muffle the sound, the audible output will likely be below ambient levels (i.e., below 50 dB from one meter).

The significant characteristics of the proposed monopropellant actuation approach for use in a high degree-of-freedom anthropomorphic arm are summarized as follows:

- Actuator power density, force density, bandwidth, and form factor suitable for the development of a high degree-of-freedom anthropomorphic arm.
- No power consumption required for isometric contraction.
- Open loop compliance and damping, coupled with backdrivability, enables natural passive limb biomechanics (e.g., free swing during gait).
- With the addition of a valve for each degree of actuation of interest, the open-loop joint impedance can be modulated independently of joint torque, which coupled with backdrivability enables interaction with both kinematically constrained and kinematically dictated tasks.
- Liquid propellant is nonflammable, insensitive to shock, has no possibility of detonation at proposed concentration levels (70-80%), and has completely safe reaction products.
- Low temperature, benign exhaust that is projected to be both visually and audibly insignificant.

These characteristics enable the development of an anthropomorphic prosthetic arm with human-like capabilities. The following sections describe the design of such an arm.

III. Valve Design

A major component necessary for the realization of the liquid-fueled arm prosthesis is the small-scale, low-power servovalve to control the gas flow rates through the actuators. Valve design was a significant issue relative to the earlier work in CO_2-powered prostheses [8,9] and continues to be a critical issue. The required characteristics of the valve for the monopropellant-powered system are low-power operation, small size, and the ability to accommodate high-temperature gases. Servovalves with such characteristics are commercially unavailable, necessitating custom design of the precision four-way servovalves. The valve design incorporates a precision ground spool/sleeve pair with a diametral clearance of 1 micron (XX gage quality) actuated by a DC motor/encoder package (Micromo model 1319T006SR-IE2-400). The valve actuation package also includes a custom cable-drive gearhead (9:1 gear ratio) that serves the dual purpose of compact gear reduction and thermal isolation due to the use of PEEK components. As such, the resulting gearhead is approximately 50% of the volume of its commercial counterpart and integrates thermal isolation with no additional components. The complete servovalve (pictured in Fig. 2 attached to the catalyst pack and manifold of the elbow joint), has a volume comparable to a AA-battery, allowing for the packaging of multiple servovalves within a small volumetric space in the arm prosthesis.

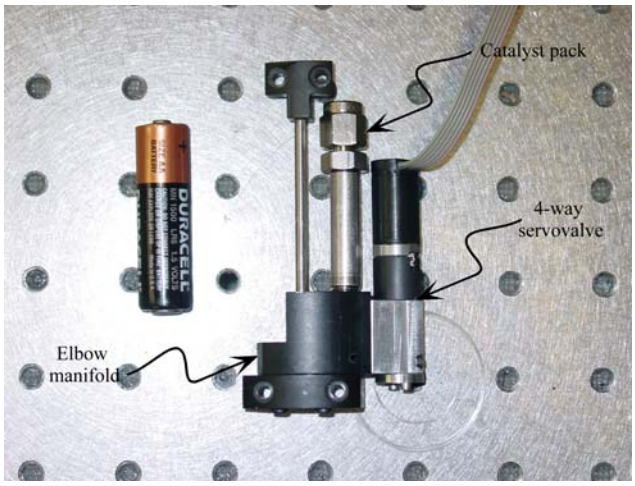

Fig. 2. Four-way servovalve attached to manifold and catalyst pack of elbow joint.

IV. Forearm Design

The first important aspect of the forearm design was sizing the pneumatic-type actuators to deliver the requisite human-like performance. The first prototype forearm was designed to deliver 50% of the output capabilities of an unaffected subject's arm. The actuator for a given prosthetic joint was chosen based on the output energy of its anatomical counterpart, which is defined by:

$$E = \tau\theta \quad (1)$$

where τ is the torque applied to the joint and θ is the angular range of motion of the joint. In conventional electromechanical designs, the power required at each joint determines the actuator size. For gas actuation, however, the energy delivered is determined by the actuator volume whereas the power is dictated by the characteristics of the servovalve controlling the flow rate of gas through the cylinder. As such, the power produced at a given joint is essentially independent of the volume of the chosen actuator. Once the required energy for a given joint is determined, the volume of the pneumatic-type actuator is then determined by:

$$V = \frac{E}{P_s} \quad (2)$$

where P_s is the supply pressure of the working gas and V is the volume of the actuator. The supply pressure for the intial prosthesis prototype is 2.1 MPa (300 psi). For elbow flexion/extension, wrist flexion/extension, and wrist abduction/adduction, an external load of 44.5 N (10 lb) was chosen to represent approximately 50% of the typical human arm load. The joint torque was then computed from the product of the external load and the joint's respective lever arm (35.5 cm for the elbow and 10.1 cm for the wrist joints). With regard to pronation/supination, the anatomical wrist was estimated to provide a torque of 4.2 Nm, as empirically determined from actuation tests of an average unaffected human subject rotating an inertial load in the presence of gravitational acceleration. Table 1 summarizes the requirements for the elbow and three wrist degrees-of-freedom.

TABLE 1
FOREARM REQUIREMENTS

DOF	TORQUE (NM)	ROM (°)	ENERGY (J)	REQUIRED ACTUATOR VOLUME (CC)
Elbow Flex/Ext	15.8	160	44.2	21
Wrist Flex/Ext	4.5	170	13.4	6.5
Wrist Abd/Add	4.5	60	4.73	2.3
Wrist Pro/Sup	4.2	150	11.1	5.3

TABLE 2
FOREARM ACTUATOR SPECIFICATIONS

DOF	STROKE (CM)	BORE (CM)	ACTUATOR DISPLACED VOLUME (CC)	ACTUATOR/REQUIRED DISPLACED VOLUME
Elbow Flex/Ext	7.6	1.9	22	1.05
Wrist Flex/Ext	5.1	1.4	7.8	1.20
Wrist Abd/Add	2.5	1.4	3.8	1.65
Wrist Pro/Sup	3.8	1.4	5.8	1.09

After computing the required volume for a given actuator, the bore and stroke of the actuator can then be determined based on the required range-of-motion, the linkage design, and the constraint that the prosthesis design should fit within the anatomical envelope of the human arm. The predominant constraint with respect to the forearm design was fitting the actuators within the available forearm length. As such, each actuator was chosen to provide the requisite energy with the smallest overall actuator length (stroke plus additional length due to endcaps/ports). Table 2 summarizes the specifications of the actuators chosen for the prosthesis forearm and shows the ratios of the actual to desired actuator volumes for each degree of freedom. This ratio provides an indirect measure of the additional actuator energy available to overcome the friction in each degree of freedom (e.g., joint friction, cylinder seal friction, etc.).

Figure 3 depicts a solid model of the elbow joint designed for the anthropomorphic arm. The elbow joint consists of a revolute joint actuated with a flat cylinder (Bimba model FO-043-3V) with a force sensor (Measurement Specialties model ELFS-T4E-100L) integrated in series with the cylinder piston rod. A custom fabricated four-way valve connects to the cylinder ports in order to control the flow of gas to and from the opposing cylinder ports. The revolute joint, shown in the exploded view of Fig. 4, is composed of an inner link sandwiched between split outer links and incorporates a potentiometer (ALPS model RDC503013A) for angular position sensing. The potentiometer is housed within the medial outer link and interfaces with the joint through a shaft pressed into the inner link. A pair of flanged

bearings (GGB model BB0604DU) provide for low-friction rotation of the revolute joint. The resulting design provides a range of motion of 105° with hard stops integrated within the split outer links of the revolute joint.

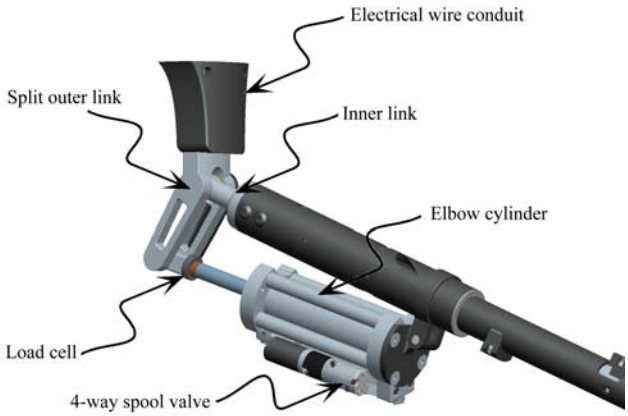

Fig. 3. Solid model of elbow joint.

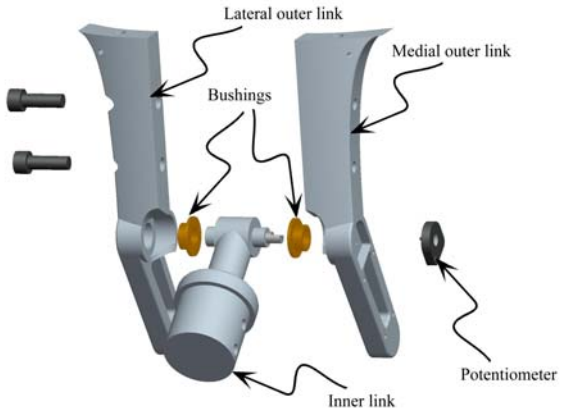

Fig. 4. Exploded view of elbow joint.

Pronation/supination of the wrist is actuated using a variant of a leadscrew assembly, the design of which is shown in Fig. 5. The design consists of proximal and distal forearms supported by a pair of flanged bearings (GGB models BB1612DU and BB1817DU) to allow rotation of the distal forearm relative to the proximal forearm (shown partially transparent) while also providing for thrust load bearing. The proximal forearm houses a potentiometer (ALPS model RDC503013A) to measure angular rotation and includes a helical slot which acts as the leadscrew in the design. The distal forearm houses a non-rotating cylinder (Bimba model 021.5-DXPV) and includes a straight slot collinear with the helical slot of the proximal forearm. A force sensor (Measurement Specialties model ELFS-T4E-100L) is connected in series with the cylinder piston rod and an orthogonally positioned PEEK crosspiece provides for relative rotation of the proximal/distal forearms. As the cylinder rod is displaced, the PEEK crosspiece slides within the helical/straight slots of the proximal/distal forearm resulting in rotation of the distal forearm relative to its proximal counterpart with a total range of motion of 95°.

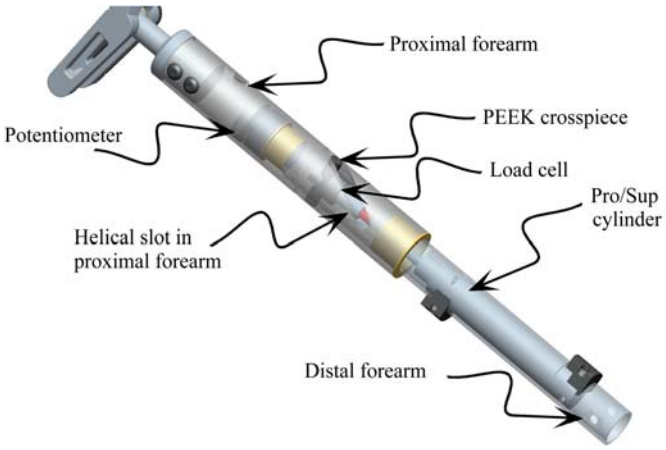

Fig. 5. Solid model of wrist pronation/supination.

Flexion/extension and abduction/adduction of the wrist, shown in the solid model of Fig. 6, is achieved with a pair of cantilevered revolute joints actuated with a pair of cylinders (Bimba models 022-DXPV and 021-DXPV). Each cylinder includes a load cell (Measurement Specialties model ELFS-T4E-100L) in series with its piston rod for force sensing in each joint. The flexion/extension cylinder has simple pinned joints at each end, but due to coupling in the cantilevered joint pair, the abduction/adduction cylinder must have spherical joints at each end. The cantilevered joint pair integrates potentiometers (ALPS model RDC503013A) and two pairs of flanged bronze bushings, as shown in the exploded view of Fig. 7. The resulting design provides a range of motion of 105° for wrist flexion/extension and 40° for wrist abduction/adduction.

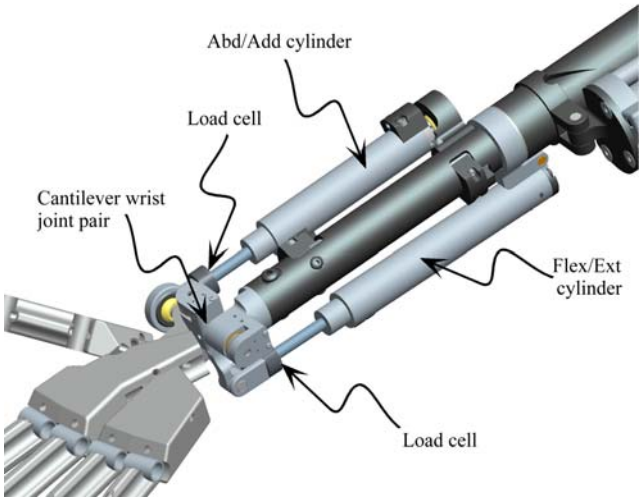

Fig. 6. Solid model of wrist flexion/extension and abduction/adduction.

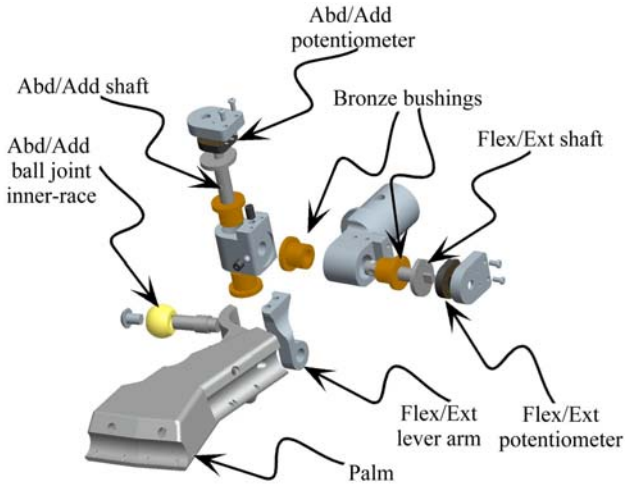

Fig. 7. Exploded view of cantilever wrist joint pair.

V. Hand Design

The anthropomorphic hand for the transhumeral prostheses has 17 coupled degrees-of-freedom driven by five degrees of actuation (Fig. 8). Pneumatic-type actuators for the hand reside in the proximal forearm, similar to native human anatomy. The pneumatic-type actuators are split with one degree for the flexion for the first finger, a second for the flexion of the second finger, the third for the flexion of the thumb, the fourth for the combined flexion of the third and forth fingers through a linear differential, and the last degree of actuation is the coupled link between thumb abduction and palm flexion, or cupping through a second differential. The interphangeal and metacarpophalangeal joints of the hand are fully compliant with no internal bearings. The primary design component of the compliant finger joints consists of opposing torsional spring pairs, as shown in the exploded finger view of Fig. 9. This paired configuration eliminates net twisting moments. Each joint has two sets of spring inserts to minimize compliance in off-axis directions. The split-tube and ring inserts serve to make each joint better approximate an ideal revolute joint by increasing the off-axis bending stiffnesses. The video accompanying this paper shows the prototype of Fig. 8 under closed-loop control demonstrating some of the hand's capabilities.

(a) (b) (c)

Figure 8. (a) An ABS prototype of the 17 degree-of-freedom hand fully extended with the use of torsional springs. (b) This prototype demonstrating a spherical grasp. (c) This prototype demonstrating a cylindrical tool grip.

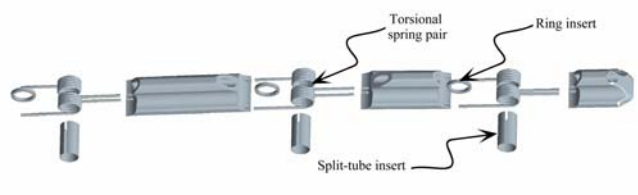

Fig. 9. Exploded view of a compliant finger.

With respect to sizing the actuation for the hand, the energy was determined based on the desired exertion force and range of motion for each finger and the thumb. For finger flexion, the energy is based on a force of 40 N over a finger-tip range of motion of 10 cm. The energy for thumb flexion is determined by a tip force of 60 N over 10 cm of motion, and that for thumb abduction/adduction is given by a force of 40 N over 8.5 cm of motion. Because of the compliance at each finger/thumb joint, the actuators must also deliver the additional energy required to deflect the torsional springs. Table 3 summarizes the requirements for the hand actuators, including both the energy (i.e., that required only of the finger/thumb) and the total energy (i.e., the finger/thumb energy plus that required for deflection of the torsional joint springs).

TABLE 3
HAND ACTUATOR REQUIREMENTS

DOF	FORCE (N)	ROM (CM)	ENERGY (J)	TOTAL ENERGY (J)	REQUIRED ACTUATOR VOLUME (CC)
Finger flexion	40	10	4.0	4.4	2.2
Thumb flexion	60	10	6.0	6.4	3.2
Thumb ab/ad	40	8.5	3.4	3.6	1.8

TABLE 4
HAND ACTUATOR SPECIFICATIONS

DOF	STROKE (CM)	BORE (CM)	ACTUATOR DISPLACED VOLUME (CC)	ACTUATOR/REQUIRED DISPLACED VOLUME
Finger flexion	3.8	1.1	3.6	1.5
Thumb flexion	3.8	1.1	3.6	1.1
Thumb ab/ad	3.8	1.1	3.6	1.6

The actuators for the hand (Bimba model 011.5-DV) are chosen based on these requirements, and the specifications are summarized in Table 4. Analogous to the cylinder specifications for the wrist and elbow cylinders, the table provides a ratio of the actual to required actuator volume as an indirect characterization of the additional energy available to overcome friction in each degree of freedom (e.g., seal and cable friction). Fig. 10 shows a solid model of the hand cylinders mounted on the distal forearm. The hand cylinders, together with the cylinders for wrist flexion/extension and abduction/adduction, form a group

seven actuators positioned radially around and mounted to the distal forearm. The actuator forces are applied through a series of cables and cable sheaths, which are equivalent to the tendons of this hand system. In order to measure cable tension, each hand actuator incorporates a load cell (Measurement Specialties model ELFM-T2E-025L) serially between the piston rod and tendon.

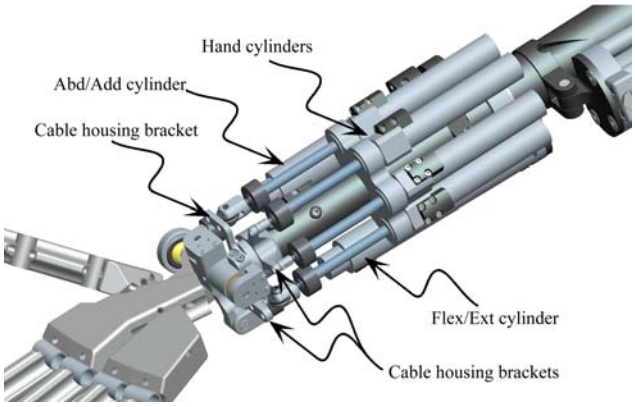

Fig. 10. Solid model of hand cylinders mounted to the distal forearm.

The designed compliance in the finger/thumb joints provides a return force to simplify the tendon actuation by passively providing an extension moment at each joint. The joint compliance also provides significant benefits with respect to hand control. In normal use, the hand will often transition between free and constrained motion. Because the joint compliance maps force input to position output, the hand will always be under force control, eliminating any instabilities associated with switching between position/force control in unconstrained/constrained motion. Two other additional assets of the compliance are insensitivity to shock loads and moderate compliance in off-axis directions. These features help to add robustness to the finger joints when interacting with the environment.

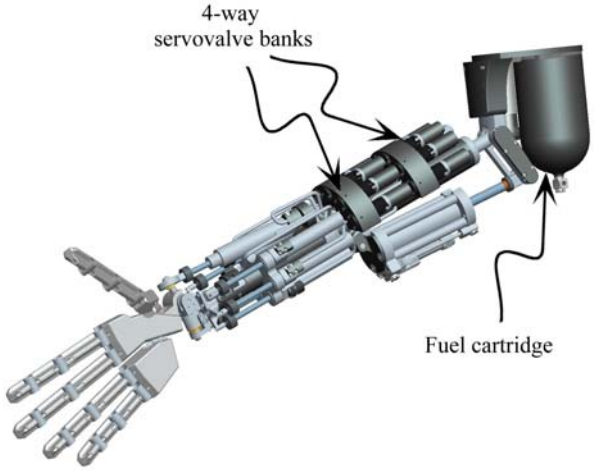

Fig. 11. Solid model of the full arm prosthesis.

VI. Conclusion

The full transhumeral prosthesis, shown in Fig. 11, incorporates the forearm and hand designs, along with nine serovalves, hot-gas delivery lines, a fuel cartridge, and on-board power/electronics. The prosthesis has a total of 21 degrees-of-freedom and 9 degrees-of-actuation, with the hand encompassing 17 degrees-of-freedom and 5 degrees-of-actuation. The fuel cartridge carries 200 mL of hydrogen peroxide, which provides 55 kJ based on 70% concentration. A volume of 105 mL is allocated for electronics and a battery for powering sensors and controlling the servovalves. The remainder of the available arm volume is reserved for the structural components for each degree of freedom and the nine servovalves. The arm is projected to weigh 17.4 N (3.9 lb), which includes the weight of all components sans the electronics, and projected to deliver approximately 50% of the force, power, and energy of an anatomical human arm.

References

[1] Goldfarb, M., Barth, E.J., Gogola, M.A. and Wehrmeyer, J.A., "Design and Energetic Characterization of a Liquid-Propellant-Powered Actuator for Self-Powered Robots.," IEEE/ASME Transactions on Mechatronics, vol. 8, no. 2, pp. 254-262, 2003.

[2] Shields, B.L., Fite, K., and Goldfarb, M. Design, Control, and Energetic Characterization of a Solenoid Injected Monopropellant Powered Actuator, *IEEE/ASME Transactions on Mechatronics*, vol. 11, no. 4, pp. 477-487, 2006.

[3] Fite, K.B., Mitchell, J., Barth, E.J., and Goldfarb, M. A Unified Force Controller for a Proportional-Injector Direct-Injection Monopropellant-Powered Actuator, *ASME Journal of Dynamic Systems, Measurement and Control*, vol. 128, no. 1, pp. 159-164, 2006.

[4] Fite, K.B., and Goldfarb, M. Design and Energetic Characterization of a Proportional-Injector Monopropellant-Powered Actuator, *IEEE/ASME Transactions on Mechatronics*, vol. 11, no. 2, pp. 196-204, 2006.

[5] Marquardt, E., "The Heidelberg Pneumatic Arm Prosthesis," *Journal of Bone and Joint Surgery*, vol. 47B, no. 3, pp. 425-434, Aug. 1965.

[6] Burrows, C.R., Martin, D.J., and Ring, N.D., "Investigation into the dynamics and control of a pneumatically powered artificial elbow," *International Journal of Control*, vol. 15, no. 2, pp. 337-352, Feb. 1972.

[7] Shen, X., and Goldfarb, M., "Independent Stiffness and Force Control of Pneumatic Actuators for Contact Stability during Robot Manipulation," Proceedings of the *IEEE International Conference on Robotics and Automation*, pp. 2706-2713, 2005.

[8] Kenworth, G. and Jolly, D.C., "Experience with the force-demand valve in controlling a pneumatically powered prosthesis," *Medical and Biological Engineering*, vol. 11, no. 1, pp. 90-94, Jan. 1973.

[9] Cool, J.C. and Pistecky, P.V., "A miniature gas-pressure valve," *Medical and Biological Engineering*, vol. 11, no. 6, pp. 771-779, Nov. 1973.